Summer 2017

The Effect of Hemodynamic Force on the Maturation of Blood Vessels during Embryogenesis

Rachel Lee Padget
Missouri State University, Padget017@live.missouristate.edu

THE EFFECT OF HEMODYNAMIC FORCE ON THE MATURATION OF BLOOD VESSELS DURING EMBRYOGENESIS

A Master's Thesis

Presented to

The Graduate College of

Missouri State University

In Partial Fulfillment

Of the Requirements for the Degree

Master of Science, Biology

By

Rachel Lee Padget

August 2017

THE EFFECT OF HEMODYNAMIC FORCE ON THE MATURATION OF BLOOD VESSELS DURING EMBRYOGENESIS

Biology

Missouri State University, August 2017

Master of Science

Rachel Lee Padget

ABSTRACT

Throughout embryonic development, blood vessels are derived from endothelial cells by way of vasculogenesis. During angiogenesis, vessels remodel to form a hierarchy of large-diameter arteries that branch into small-diameter capillaries. In this maturation, vessels respond to unidentified signaling events to become surrounded with an outer layer of vascular smooth muscle cells (vSMCs). This results in arteries that have a thick vSMC layer, veins that have a thin vSMC layer, and capillaries that have a very thin or absent vSMC layer**.** What remains to be determined is the cause of the thicker layer of vSMCs around proximal arteries. Previous studies have implicated that mechanical forces provided by blood flow control the growth of arteries over capillaries. I hypothesize that these mechanical forces also determine the extent of vSMC coverage. To test this, I compared the extent of vSMC in arteries of normal-flow mouse embryos (wild type) with those in reduced-flow embryos (*Myl7* [-/-] mutant). I observed less vSMC coverage in the proximal arteries from reduced-flow embryos versus normal-flow embryos. With immunostaining and confocal imaging, I determined that the amount of vSMCs did not differ between reduced-flow and normal-flow tissues. Reduced-flow tissues exhibit a failure of the vSMCs to migrate away from capillaries towards proximal arteries, and a failure to surround the arteries. My findings provide evidence that hemodynamic force is required for vSMC recruitment, but not for vSMC differentiation or proliferation.

KEYWORDS: Vascular smooth muscle cells, vessel maturation, vascular development, angiogenesis, hemodynamic force

This abstract is approved as to form and content

_____

Ryan Udan, PhD
Chairperson, Advisory Committee
Missouri State University

THE EFFECT OF HEMODYNAMIC FORCE ON THE MATURATION OF BLOOD VESSELS DURING EMBRYOGENESIS

By

Rachel Lee Padget

A Master's Thesis
Submitted to the Graduate College
Of Missouri State University
In Partial Fulfillment of the Requirements
For the Degree of Master of Science, Biology

August 2017

Approved:

_____
Ryan Udan, PhD

_____
Laszlo Kovacs, PhD

_____
Paul Durham, PhD

_____
Julie Masterson, PhD: Dean, Graduate College

ACKNOWLEDGEMENTS

I would like thank Dr. Ryan Udan for all of his help and guidance in my academic career and professional development here at MSU. In addition, I wish to acknowledge Dr. Laszlo Kovacs and Dr. Paul Durham for their assistance and knowledge as part of this thesis committee and as professors. I also want to thank and acknowledge my lab mates for their assistance throughout this project: Samantha Frederickson, Shilpa Mohite, and Tanner Hoog. For assistance with flow cytometry, I would also like to thank Dr. Chris Lupfer. For funding, I wish to thank the Missouri State Biology department and the Missouri State Graduate College. Finally, yet importantly, I wish to thank my family and friends for their support throughout this process.

TABLE OF CONTENTS

LIST OF TABLES

LIST OF FIGURES

INTRODUCTION

The cardiovascular system is comprised of a heart and blood vessels, and it is the first functional organ system formed during embryonic development in mammals (Moore and Metcalf, 1970), In the very early mammalian embryo, the cardiovascular system is not required, as the embryo is small enough to rely upon simple molecular diffusion from the surrounding maternal fluids/tissues. However, as the embryo grows, a functional cardiovascular system is vital for the exchange of nutrients, gases, and waste products. To set up this system, the embryo has the challenge of creating a hierarchical, branched blood vessel tree, with large vessels connected to the heart, which connect to smaller vessels far away from the heart. This is an important physiological adaptation for proper oxygen exchange and for the efficient movement of blood. The establishment of this complex vascular pattern is regulated by a series of cues that promote blood vessel growth and development by several mechanisms: vasculogenesis, angiogenesis, artery/vein specification, and vascular maturation.

Vasculogenesis

Vasculogenesis is the *de novo* development of new vessels from an aggregation of endothelial cell precursors (angioblasts). Though the first blood vessels form during vasculogenesis, this process can occur at various stages throughout an organism's life. Before vasculogenesis can occur, mesoderm tissue must form first, ultimately allowing for angioblasts to emerge from a subset of the mesoderm. The mesoderm originates during gastrulation when the primitive streak forms and elongates, and differentiating

mesoderm cells ingress between the epiblast and primitive endoderm layers in a process called epithelial-to-mesenchymal transition (EMT). This occurs at E6.0-6.5 (Embryonic day—7 days after fertilization) in mice (Ichikawa et al., 2013). Upon EMT, epiblast cells downregulate epithelial genes, such as *E-cadherin*, and upregulate other genes that gives them the ability to migrate. Subsequently, they acquire mesenchymal markers such as N-cadherin (Ferrer-Vaquer et al., 2014). As cells from the epiblast migrate into the embryo, all three germ layers of the mouse embryonic and extraembryonic tissue are present: endoderm, mesoderm (embryonic and extraembryonic), and ectoderm (Kovacic et al., 2012).

Vasculogenesis first starts in an extraembryonic tissue, called the yolk sac, where blood vessels arise from a subset of extraembryonic mesoderm to give rise to primitive yolk sac vessels E7.0 (Drake and Fleming 2000). Here, hemangioblasts (blood/endothelial multipotent progenitor cells) arise from a subset of the extraembryonic mesoderm. These cells collect together to form a structure called the "blood islands". Hemangioblasts of the blood islands then begin to differentiate into angioblasts (endothelial cell precursors) and hematopoietic cells (blood cell precursors). Immediately after, the angioblasts form tubes to encapsulate the hematopoietic cells, and these tubes connect with other tubes to create the primitive capillary plexus of the yolk sac (Moore and Metcalf, 1970) (Schmidt et al., 2007). The capillary plexus is a network of primitive blood vessels that do not have any obvious hierarchies, as the capillaries are all interconnected and have similar diameters. The formation of the capillary plexus relies heavily on the activations of the Vascular Endothelial Growth Factor (VEGF) signaling pathway (Ferguson et al., 2005). VEGF acts to regulate endothelial cell differentiation,

migration, proliferation, and blood vessel branching patterns. Ultimately, VEGF activation leads to the further differentiation of angioblasts into endothelial cells that now express other endothelial markers (*Pecam1*, *Tek*, *Laminin* and *Tal*).

Slightly later (E7.3), the dorsal aortae (paired embryonic blood vessels) forms from the connection of embryonic mesoderm-derived angioblasts to form a pair of vessels that extend from the heart towards the posterior tail of the developing embryo (Drake and Fleming, 2000). In the early embryo (E7.3), blood cell production exclusively occurs in the yolk sac. By E7.8-E8.0, the yolk vessels connect to the heart, and the heart connects to the dorsal aorta, and this connects back to the yolk sac vessels; thus forming a circulatory loop.

Angiogenesis overview

The formation of new blood vessels from preexisting vessels is called angiogenesis. This is accomplished through several different mechanisms, which also leads to the development of blood vessel hierarchy. Angiogenesis occurs not only in development, but during wound healing, hypoxia of tissues, and tumor growth in adult tissues (D'Alessio et al., 2015).

During mouse development, angiogenesis begins at E8.5 in the newly formed capillary plexus. Blood vessel formation occurs via four different mechanisms: sprouting, fusion, intussusception, and regression. Sprouting is the most common mechanism used during angiogenesis as well as in in adult tissues. A vessel can sprout from a pre-existing vessel by a signal (VEGF) from the surrounding tissue. Specifically, an endothelial cell of a blood vessel that is exposed to the highest amount of VEGF will become an

endothelial tip cell. Tip cells are capable of growing/sprouting out of the vessel. Specified tip cells then communicate to adjacent endothelial cells of the blood vessel via Dll4 (Delta like ligand 4)-induced Notch signaling. This provides two functions: 1) to proliferate and provide more stalk cells behind the tip cells to grow out the sprout, and 2) to downregulate the Vegf receptor so that the stalk cells do not become tip cells themselves (D'Alessio et al., 2015). Another angiogenesis mechanism is blood vessel fusion. Newly formed vessels will fuse to neighboring vessels. This can be done between two parallel vessels to create a larger vessel (Udan et al., 2013a), and it could be done at the tip of vessels to connect vessel sprouts together. It is known that macrophages aid in blood vessel fusion by secreting VEGF-C to induce tip cell fusion (Tammela et al., 2011). Regression is the pruning of blood vessels to eliminate supernumerary vessels, and to refine vessel branching patterns. Notch/Dll4 signaling has also been shown to play an important role in vessel regression (Korn and Augustin, 2015). The last known mechanism of angiogenesis is intussusception, which is the angle change of blood vessels. This form of angiogenesis is the least common, but has been detected in rodent lung capillaries, and in chicken chorioallantoic vessels (Kurz et al., 2003). Intussusception involves the formation of an endothelial pillar through the middle of a vessel, and the expansion of that pillar, changing the angling of the vessel (Herbert and Stainier, 2011).

Angiogenesis: vascular remodeling

All four mechanisms of angiogenesis play an important role in building new vessels from preexisting vessels, but also in patterning the new vessels to create

hierarchies and unique branching patterns. This later concept is named vascular remodeling, which primarily acts by regulating vessels diameters to create the hierarchy. Thus, vascular remodeling contributes to the formation of large-diameter arterial vessels, which carry blood away from the heart, and large-diameter venous vessels, which carry blood back towards the heart.

Hemodynamic force regulates vascular remodeling. For a decade, it has been known that hemodynamic force (force that blood flow exerts on a blood vessel) acts as a signal to promote the remodeling of the vasculature. For example, loss-of-function of the *Myosin light chain 7* (*Myl7*) gene, also known as *Myosin light chain 2* (*Mlc2a*), specifically impairs the ability of the atria of the heart to contract, leaving only the left and right ventricles to pump blood (Huang et al., 2003). This produces a reduced blood-flow mouse embryo model (called reduced-flow) that results in a lack of vascular remodeling (even though vessels do not express *Myl7*). Studies have confirmed that this defect in remodeling was due to a lowering of hemodynamic force because experimental removal of blood cells from circulation, in cultured embryos, lowers fluid viscosity. This also reduces hemodynamic force, resulting in a lack of vascular remodeling (Lucitti et al., 2007). However, if these same embryos are injected with hetastarch to increase plasma viscosity, the vascular remodeling phenotype is recused, providing evidence that hemodynamic force regulates remodeling. Moreover, subsequent studies have confirmed that vessels exposed to high hemodynamic force undergo vessel-diameter increase by the fusion of neighboring vessels together; whereas, vessels exposed to low hemodynamic force remain as small-diameter capillaries (Lucitti et al., 2007); (Udan et al., 2013a). In

summary, it is clear that hemodynamic forces play a crucial role in the development of vessels.

Artery/venous specification. There are certain molecular markers that specify endothelial cells to become endothelial vein or endothelial artery cells, but this varies by location. In the mouse yolk sac plexus, *EphrinB2* is involved in the determination of arterial endothelial cells; whereas, *EphB4* is involved in the determination of venous endothelial cells (Shin et al., 2001). Also, Notch signaling (Delta-like ligand 4 and Jagged2) helps specify arterial endothelial cells; whereas venous endothelial cells are controlled by CoupTFII (You et al., 2005). In the intraembryonic tissue, artery and vein genes are present but at different time points. *Efnb2* and *Notch* related genes (*Hey1, Hey2*, *Dll4*, *Notch1* and *Notch4*) are expressed first in artery-fated endothelial cells and then venous-fated endothelial cells (Corada et al., 2014).

Though arterial and venous markers become expressed prior to the onset of flow, other evidence suggests that flow plays an important role in the maintenance of arterial/venous gene expression. In chick embryos, the expression of *EphrinB2* (arterial marker) is dependent on flow and is not activated without the presence of blood flow (le Noble et al., 2004). In the murine model, *Neurophilin1* (*Nrp1*) plays a vital role in capillary plexus patterning, but loss of flow downregulated *EphrinB2*, which is also impacted by loss of *Nrp1* (Jones et al., 2008).

Blood vessel maturation

Blood vessel maturation occurs after vessels remodel. This process occurs to create a stable, mature vessel through the recruitment of mural cells to the recently

remodeled endothelium layer. The term mural cell refers to both vascular smooth muscle cells (vSMCs) and pericytes (Gaengel et al., 2009). Vascular smooth muscle cells collectively wrap around large vessels as a tissue layer; whereas, pericytes are individual cells that wrap around single capillaries.

In adults, vascular smooth muscle cells form a tissue layer called the tunica media, which functions to regulate contractile tone, and hence blood flow in adult vessels. The tunica media thickness varies in different tissues, which is dependent on the function of that tissue. The arteries contain a very thick tunica media that helps to counteract the strong pressure of oxygenated blood that is pumped throughout the entire body. Veins contain the second thickest tunica media because the pressure of the deoxygenated blood is reduced. However, capillaries have only a one-cell thick endothelium, occasionally covered by single pericytes, or no tunica media at all (West, 2000). The reason for the reduction in vSMCs in capillaries is to enhance tissue oxygenation. Lessons learned about embryonic vSMCs can likely still apply to adult vSMCs because these cells are quite plastic and can detach from vessel walls, undergo proliferation and migration, and reattach/redifferentiate into a stable form. This plasticity, called phenotypic modulation, can occur in adult vessels upon injury, disease or growth of new vessels (Jacot and Wong, 2008).

Since developing vessels are initially devoid of mural cells, understanding mural cell origin may provide insight into their subsequent coverage of the endothelium. Mural cells (vSMCs and pericytes) differentiate from various embryonic and extraembryonic tissues, such as the neural crest, lateral plate mesoderm, and somatic/paraxial mesoderm (Armulik et al., 2011). The main transcription factor that is required for the

differentiation of mural cells from these tissues is serum response factor (SRF). However, SRF is expressed ubiquitously throughout all cells during development, so there must be other mechanisms to precisely control which cells become mural cells (Barron et al., 2005). Factors that may provide tissue-specificity of mural cell differentiation are the transcriptional coactivators of SRF: Myocardin, MRTF-A, and MRTF-B. These cofactors are also required for vSMC differentiation, as loss of these genes in mice leads to in a failure of vSMCs to differentiate, and overexpression of these cofactors in non-vSMCs results in the induction of vSMC markers (Mack et al,. 2011). Myocardin, MRTF-A and MRTF-B may allow SRF to function in a tissue-specific manner in a subset of mesoderm and neural crest cells because MRTF-A and MRTF-B are highly expressed in vSMCs, and Myocardin is detectable in vessels.

In the early yolk sac, when vessels are being remodeled (between E8.5 and E9.25), the tissue is completely devoid of vSMCs, and by E9.5 the vSMCs arise from the mesoderm, and quickly begin to surround the vessels. It is unclear how genes such as *Mrtf-A*, *Mrtf-B* and *Myocardin* become upregulated in a subset of this mesoderm. Studies have implicated *Notch2, Notch3*, *Pdgf-β*, and *Tgf-β* to act upstream of the transcriptional coactivators to control their differentiation (Mack et al. 2011). However, whether these same factors control vSMC coverage around vessels is unclear, because in addition to controlling vSMC differentiation, they have also been shown to regulate vSMC proliferation and recruitment. Therefore, it is unclear exactly how these factors influence the cellular behaviors of vSMCs during the maturation process. Thus, more studies need to be done to elucidate the role that vSMC differentiation, proliferation, or recruitment play in vessel maturation.

Even if *Notch2, Notch3, Pdgf-B* and *Tgf-B* regulate vascular coverage, it is challenging to understand why only the large proximal vessels are capable of having the highest vSMC coverage. Previous studies have implicated that every capillary of the yolk sac that receives high-hemodynamic force is capable of forming the large proximal vessel. This lends itself to the idea that hemodynamic force is also required for determining the extent of vSMC coverage during maturation. Insight into the role of hemodynamic force in regulating vSMC coverage may have important implications for human health and disease, as there are many diseases associated with the thinning of vessel walls.

Human significance

Improper thickness of vessel walls can lead to a variety of health problems in humans, from a bulging of vessels known as a hemangioma or birthmark to congenital brain aneurysms. Congenital vascular malformations (CVMs) occur in roughly 1% of all live births in the United States and can affect arteries, veins, and lymphatic vessels in children (Eerola et al., 2003). CVMs have many different forms of presentation, all with varying impacts on health, which ranges to nearly unnoticeable to life threatening. Arteriovenous fistula (or shunting) is the abnormal connection between veins and arteries that can lead to swollen veins and arteries, decreased diastolic pressure, and an increased burden on cardiac output (Liberthson et al., 1979). Children can be born with this condition in a variety of places throughout their body, from the thoracic cavity to limbs. Despite the frequent occurrence of these conditions, as of now, there is no explanation for these phenomena (Jabari et al., 2016).

Congenital arteriovenous aneurysms are rare but deadly when they occur in the brain. Between 1939 and 2011, roughly 1200 cases of non-traumatic pediatric brain aneurysms were reported (Sorteberg and Dahlberg, 2013). The causes of the aneurysms are unknown, and many are unrelated to any disease. Hemorrhaging of the thinning vessels usually occurs several years after birth. Many children have giant aneurysm events when compared to adults, and their hemorrhaging events repeat throughout their lifetime (van Rooij and Sluzewski, 2009). It has been reported that the mortality rate of children with hemorrhaging events is as high as 50%. Follow-up studies and studies discussing neurological functionality after an event are sparse due to many of the patients in the initial study dying before completion of follow-up exaninations (Kakarla et al., 2010).

Because of the variety of congenital vascular malformations and the reduced lifespan of children born with them, it is important to understand the causes of these CVMs. Many causes of CVMs are unknown and thus, treatments are reactive rather than preventative. Development of treatments could include a drug to thicken vessel walls to prevent repeated hemorrhaging events in congenital aneurysms patients.

Hypothesis and goals

My study begins to investigate whether hemodynamic force impacts the maturation of blood vessels by affecting the coverage of vSMCs around large proximal vessels. As previously stated, mouse embryos subjected to low hemodynamic force display impaired vascular remodeling (Lucitti et al., 2007). In these embryos, proximal vessels fail to undergo an expansion in diameter that is normally found at the top of the vessel

hierarchy. In our preliminary studies, I sought to assess whether hemodynamic force similarly affects vSMC coverage during maturation. I found that proximal arteries and veins exhibited a high and medium level of vSMC coverage, respectively. This correlated to differences in flow regimes in proximal arteries and veins, as previously published (Udan et al., 2013b). Further, I also determined that reduction of hemodynamic force resulted in diminished vSMC coverage in proximal vessels, resulting in a coverage observed similar to that in distal capillaries of normal-flow embryos. Thus, hemodynamic force must be controlling vSMC coverage, but the cellular mechanism for this loss of coverage is unknown. I proposed two hypotheses to explain this loss of coverage upon reduced hemodynamic force:

1. Hypothesis one: Hemodynamic force promotes the localized proliferation and/or differentiation signals of vSMCs.
   In this hypothesis, hemodynamic force may affect the number of vSMCs by promoting the localized proliferation or differentiation of vSMCs around vessels of high-flow. Here localized proliferation/differentiation would be followed by immediate adhesion around the nearby vessels without much vSMC migration (Fig. 1).
2. Hypothesis two: Hemodynamic force promotes the recruitment of vascular smooth muscle cells.
   In this hypothesis, hemodynamic force does not regulate the number of vSMCs. Instead, it regulates the recruitment of vSMCs towards areas of high hemodynamic force (Fig. 2).

MATERIALS AND METHODS

Mouse care and lines

This study used animal subjects and prior approval for this project was obtained from the Missouri State University Institutional Animal Care and Use Committee (November 20, 2014; approval #15-004.0-A, December 01, 2014; approval #15-008.0-A). Housing and procedures involving the mice met the requirements of National Institute of Health animal care and use guidelines. Adult *Myl7/Mlc2a* (referred to as *Myl7* in this study) (Huang et al., 2003) and *Myl7;CD1-Tg(sma-mCherry)* (Armstrong et al., 2010) mice were bred in the animal vivarium. All mice were housed in Ancare standard mouse cages at a temperature of 20.0-23.0 °C and under a diurnal cycle of 12-h light/ 12-h dark, and had *ad libitum* access to water and Purina Labdiet 5001 (Purina) when not in experimental use or Purina Formulab diet 5008 (Purina) when used for breeding and experiments. Female and male mice used for experiments ranged 2-to-12 months in age.

Myl7/Mlc2a (Huang et al., 2003*)* and *Myl7;CD1-Tg(sma-mCherry)* (Armstrong et al., 2010) embryos were used for immunohistochemistry whole yolk sac experiments. *Myl7* embryos and yolk sacs were used for flow cytometry experiments. *Myl7;CD1-Tg(sma-mCherry)* embryos and yolk sacs were used for whole yolk sac immunohistochemistry experiments. Determination of embryonic day was measured after a noticeable vaginal plug present in the afternoon, marking that time point as E0.5.

Whole yolk sac immunohistochemistry

Adult pregnant mice were euthanized in a plastic container via CO_2 inhalation followed by cervical dislocation. Whole embryos were isolated at E10.5 in cold Phosphate Buffer Saline (PBS). The uterine muscle and decidua were removed to expose the intact yolk sac. A small hole was cut into the top of the ectoplacental cone to ensure exchange of buffer in and out of the yolk sac.

Embryos were fixed in 4% paraformaldehyde (PFA) in polypropylene round-bottom tubes while rotating on a nutator for 35 minutes. Embryos were washed 3 times for 5-10 minutes each using PBS while shaking at room temperature. Then, the embryos were given a final 5-10 minute wash using PBS containing 0.1% Triton (PBT) while shaking at room temperature. Embryos were then washed in blocking buffer of 5% Normal Donkey Serum (NDS; Sigma D9663-10mL), 1% Bovine Serum Albumin (GE Healthcare Life Science SH30574.01) (BSA), in PBT for 1.5 hours at 4° C while shaking. Embryos were then incubated for 48 hours in primary antibody with Serum Buffer Triton (2.5% NDS in PBT) (SBT).

Primary antibodies used for these experiments and what they label are listed in Table 1. Embryos were then washed several times in SBT over the course of one day to be incubated in secondary antibody in SBT for 48 hours at 4° C while shaking. The secondary antibodies used for these experiments and what they label are listed in Table 1. Embryos were then washed in SBT 4 times by shaking at 4° C for 20 minutes, and the last wash was done with PBS. The yolk sac was dissected open to display the arterial tree on the right and venous vein on the left, and was mounted onto plain 3” x 1” x 1 mm

microscope slides (Fisher Scientific 12-544-1). Slides were then imaged using confocal microscopy. The embryos were saved for genotyping.

Quantification of vSMC total number and vSMC undergoing mitosis

Myl7;CD1-Tg(sma-mCherry) yolk sacs from E10.5 embryos were isolated, stained with PH3 antibody or Kdr antibody and Sma antibody, and yolk sacs were flat mounted on plain slides. Confocal images of endothelial, vascular smooth muscle, or mitotic cells were taken using Olympus IX81-ZDC inverted fluorescence microscope with the Slidebook 6.0 software. For area analysis of vSMCs in the distal capillary regions, 5 *Myl7* (+/+) & (-/-) yolk sacs and 4 *Myl7* (-/-) yolk sacs were imaged. For area analysis of mitotic cells and vSMC total, 7 *Myl7* (+/+) & (+/-) yolk sacs were imaged and 4 *Myl7* (-/-) yolk sacs were imaged. A random sample of 10 images (10 slices at 2.2 μm for each image) were taken across different regions of each yolk sac using spinning disc confocal EM-CCD digital camera, and a projection of the Z-stack was made to produce a single image.

Quantification of the amount of vSMCs present in capillary regions of the yolk sac was not possible because cell boundaries were not apparent. As a result, two or more cells that overlap may appear as one cell. Thus, to quantify the amount of vSMCs that occupy capillary regions, the percent area occupied by vSMCs divided by total surface area was determined in reduced-flow yolk sac samples *Myl7(*-/-) and normal-flow yolk sac samples *Myl7(*+/-). This was done by binarizing the image using Adobe Photoshop so that all vSMCs were black and the background tissue was white. The percent area that the vSMCs occupied was measured using ImageJ. Statistical analysis was done using a

Student's t-test in Microsoft Excel. For quantification of vSMC undergoing mitosis, PH3, Sma double positive cells were quantified. These can be quantified as single cells, as the PH3 labeling is distinct and does not overlap with other PH3-stained nuclei. These values were then divided by the percent area occupied by the total vSMCs to give an estimate of the amount of mitotic vSMCs in reduced-flow and normal-flow yolk sacs.

Flow cytometry/quantification of total cells and vSMCs

Total cell count and total vSMC count was analyzed using flow cytometry of *Myl7* (-/-) and *Myl7* (+/-) embryo or yolk sac tissue. Whole embryos with yolk sacs were isolated in cold Hank's balanced salt solution with calcium chloride and magnesium chloride (HBSS+) (Fisher Scientific) at E10.5 and the uterine muscle and decidua were discarded. Both mutant and wild-type tissues were used and kept in 300 µL HBSS+, separated based on phenotype. The embryos were separated from the yolk sac and saved for analysis, the tails were cut to be used for genotyping. The tissue types used in this experiment are listed in Table 2.

Cells were centrifuged at 300g for 30 seconds then media was replaced with Type II 0.2% collagenase (Thermo Fisher Scientific, #17101015). Degradation of collagen was done by incubating cells in 37°C incubator and by sequential pipetting with a pipette tips of decreasing size (1000 µL, 200 µL, 10 µL) and finally with a 25 G x 38mm hypodermic needle (Fisher Scientific, #14-826-49). Cells were filtered using a 40 µm cell strainer (Fisherbrand), centrifuged at 300g for 10 minutes, after the removal of the medium and fixed in 100 µL 2% PFA for 5-20 minutes (depending on experiment) on ice. Cells were centrifuged at 300g for 10 minutes, media removed, then incubated in 100 µL 1x

Permwash (Biolegend) and 2.5% NDS for 10 minutes on ice. Then, cells were centrifuged at 300g for 10 minutes, after the removal of the medium, the cell pellet was resuspended in 100 µL 1x Permwash (with or without 1:200 SmaCy3 antibody), and incubated for 15 minutes at room temperature. For flow cytometry analysis, cells were centrifuged at 300g for 10 minutes then placed in 100 µL 1x Permwash and quantified in a BD Accuri C6 Flow Cytometer. Samples were run through on unlimited events, for a maximum of 1,000,000 events that included forward side scatter over 10,000.

Parameters on the C6 software were chosen based on repeated trials of control autofluorescence yolk sacs and embryos without the Sma-Cy3 antibody as compared to fluorescence of samples with the Sma-Cy3 antibody. This allowed for comparison of the cells natural fluorescence with the fluorescence that occurs upon addition of the Sma-Cy3 antibody. Cells with background fluorescence were removed from counts by selecting the forward scatter gate of registering events that fluoresce at 10^4 or higher.

Tail cuts/DNA isolation

Juvenile and adult mice had tail cuts performed for genotyping. Juvenile tail cuts were performed without anesthesia and used for DNA isolation. Adult mouse tail cuts were performed with 3ppm isoflurane until mice were unconscious, then tails were clipped. 200 µL of tail buffer (1 mL of 5M NaCl, 2.5 mL of 1M Tris pH 8.0, 10 mL of 0.5M EDTA pH8.0, 5 mL of 10% SDS, q.s. 50 mL) was added to the tail clip with 10 µL Proteinase K (Thermo Scientific) and incubated for 24 hours at 55°C. The solution was briefly mixed by flicking the tube to finalize resuspended tissue and 200 µL of phenol chloroform was added. The tubes were then gently mixed by shaking up and down 20-30

times and centrifuged for 10 minutes at 13.3 g at room temperature. Subsequently, the aqueous phase was transferred to a clean microcentrifuge tube, and the organic phase was discarded. An equal amount of 100% isopropanol was added, mixed, and then centrifuged at 13.3g for 10 mins. The solution was removed by decanting, the pellet was washed in 500 µL of 70% ethanol, and centrifuged at 13.3 g for 10 minutes. The ethanol was decanted and the tubes were left to dry upside down on a tissue. The DNA was suspended in 75 µL of distilled water was 24 hours at 4°C.

PCR genotyping

DNA extracted from embryonic tails were used for genotyping to validate phenotypic expression. Purified embryonic DNA was amplified using Pro-Taq DNA polymerase (Deville Scientific, Inc) and the following primers (5' – 3'): wild-type band, *Myl7*-wt-F (GGCACGATCACTC) and *Myl7*-wt-R (ATCCCTGTTCTGG); mutant band, *Myl7*-mut-F (ACAGGGAATCACA) and *Myl7*-mut-R (CGAACCTGGTCGA). PCR cycles consisted of denaturing at 95.0°C for 5 minutes, then 35 cycles of denaturing at 95.0°C 30 seconds, annealing at 56.5°C 30 seconds, and extension at 72.0°C 1 minutes, and a final extension at 72.0°C for 5 minutes.

Table 1. Antibodies used in my study.

Antibody	Experimental Procedure	Dilution	Company	Incubation Period
Anti-vascular endothelial growth receptor 2, made in goat	Whole Yolk Sac (both)	1:200	Abcam	48 hours
Anti-alpha smooth muscle actin-Cy3, made in mouse	Whole Yolk Sac (both), Flow Cytometry	1:1250, 1:250	Sigma Sciences	48 hours
Anti-histone H3, made in rabbit	Whole Yolk Sac (Mitosis count)	1:500	Abcam	24 hours
DAPI, made in mouse	Whole Yolk Sac (vSMC count)	1:500	Sigma Sciences	48 hours
Alexa Fluor 488 donkey anti-goat	Whole Yolk Sac (vSMC count)	1:500	Life Technologies	48 hours
Alexa 568 donkey anti-rabbit	Whole Yolk Sac (mitosis count)	1:500	Life Technologies	24 hours
Alexa Fluor 488 donkey anti-rabbit	Whole Yolk Sac (mitosis count)	1:500	Life Technologies	48 hours

Table 2. Tissues used in quantification of total cells and vSCMs

Tissue Type	Amount	Genotype	Antibody
Embryo	1	Wild-type	None
Yolk Sac	2	Wild-type	None
Embryo	1	Mutant	None
Yolk Sac	2	Mutant	None
Embryo	1	Wild-type	Anti-alpha smooth muscle actin-Cy3
Yolk Sac	2	Wild-type	Anti-alpha smooth muscle actin-Cy3
Embryo	1	Mutant	Anti-alpha smooth muscle actin-Cy3
Yolk Sac	2	Mutant	Anti-alpha smooth muscle actin-Cy3

PRELIMINARY DATA

vSMC coverage is reduced in yolk sac vein and capillaries compared to artery

As mentioned above, adult blood vessels exhibit a difference in vSMC coverage between arteries, veins, and capillaries, with arteries having highest vSMC coverage. Since I are interested in understanding what controls vSMC coverage, I sought to determine if the same difference in thickness is apparent during embryonic development. Yolk sacs from E10.5 embryos were used, as the vasculature is well developed and vessels have matured. For example, the arterial tree exhibits regular branching into smaller primary and secondary branches; the vitelline vein displays two main vessels; and the capillary region connects the arteries and veins. These vessels have already initiated maturation only one day earlier (at E9.5), and by E10.5 stable, mature blood vessels have formed.

To observe if there was a vSMC coverage difference between yolk sac arteries, veins, and capillaries, whole-mount immunostaining and confocal microscopy was used. The proximal artery showed complete vSMC coverage around the inner lining of the vessel— comprised of endothelial cells (Fig. 3A-C). In comparison, the vein showed vSMC coverage around the vessel, however, the fluorescence signal was not as strong as in the artery (Fig. 3D-F). Also, vSMC coverage was the most dramatically reduced in the capillary region of the mouse yolk sac (Fig. 3G-I). These data reveal that the extent of vSMC coverage is similar to what is observed in the adult, even at this very early stage of maturation.

Interestingly, the amount of vSMC coverage correlated to the levels of hemodynamic force, as previously measured in proximal arteries, veins, and capillaries of yolk sacs (Udan et al. 2013). Considering that hemodynamic force has been shown to regulate vessel hierarchy, I sought to determine if hemodynamic force is similarly required for controlling the amount of vSMC coverage.

Vascular smooth muscle layer is reduced with low hemodynamic force in the yolk sac proximal artery and the dorsal aorta

To determine whether hemodynamic force impacts the maturation of blood vessels, I analyzed vSMC coverage in *Myl7* reduced-flow mutant (-/-) and normal-flow control (+/-) embryonic yolk sacs. The yolk sac vasculature in normal-flow arteries displayed a large diameter vessel comprised of endothelial cells and a complete coverage of vSMCs (Fig. 4A-C). However, the proximal artery of the yolk sac in reduced-flow embryos showed poor vessel development, and minimal vSMC coverage of the vessel (Fig. 4D-F).

Next, I sought to determine if this phenotype was similarly found in intraembryonic vessels. Though the capillary network is still growing in E10.5, the most prominent vessel of the embryo, the dorsal aorta, is functional. The challenge to imaging these vessels is that it is internal, thus, it could not be imaged by a whole-mount approach, due to light scattering issues, thus, I performed cross sections. E10.5 normal-flow dorsal aorta cross sections showed robust vessel development of the endothelial cells and complete vSMC coverage around the vessel (Fig. 4G-I). Similar as the reduced-flow yolk sac vasculature, the reduced-flow dorsal aorta also exhibited reduced vessel

development and almost no vSMC coverage around the vessel (Fig. 4J-L). These results reveal that reduction of hemodynamic force does not impact blood vessel formation, but does impact its maturation.

RESULTS

Low Hemodynamic Force does not impact the Proliferation and Differentiation of vSMCs

It is clearly evident that hemodynamic force regulates that amount of vSMCs that surround the yolk sac and embryonic arteries, and I similarly saw this disparity in reduced-flow proximal veins (data not shown). To explain this phenotype, two hypotheses were formulated: 1) hemodynamic force regulates the localized proliferation/differentiation of vSMCs (which later surround the closest vessels), 2) hemodynamic force regulates the recruitment of vSMCs to the high-flow, proximal vessels (without affect the differentiation/proliferation status of the cells) (Fig. 1).

To determine whether vSMC proliferation was influenced by reduction of hemodynamic force, I stained normal-flow and reduced-flow yolk sac tissue with a mitotic antibody marker (phospho-Histone H3 [PH3]) and co-labeled with a vSMC antibody marker (Smooth muscle alpha actin [Sma]). PH3 cells were easily identified and counted: however, vSMCs could be visualized, this was a cytoplasmic marker. It was difficult to determine whether two vSMCs that were adhered together where separate cells or the same cell. Thus, I quantified total PH3-labeled cells and divide this number by the total surface area occupied by vSMC staining to determine a mitotic index. After comparing the mitotic index in normal-flow vs. reduced-flow embryonic yolk sacs, I observed no difference in proliferation—suggesting that hemodynamic force does not affect the proliferation status of vSMCs (Fig. 5I).

Though this data indicates that hemodynamic force does not impact global levels of proliferation, perhaps it affects the ability for vSMCs to differentiate. One strategy to determine whether there is an altered differentiation status is to assess changes in vSMC differentiation markers. Thus, I sought to determine if expression of the vSMC differentiation marker, *Mkl2* (Mokalled et al., 2015), was altered upon reduced-flow. However, qRT-PCR of *Mkl2* in normal-flow versus reduced flow E10.5 yolk sacs revealed no significant difference in global expression patterns of Mkl2 (data not shown). One caveat to this experiment is that there could be minute differences in gene expression that are not detectable by qRT-PCR, but perhaps reduced-flow yolk sacs still exhibit diminished vSMC differentiation. In this case, flow could still impact the total number of vSMCs available to cover vessels.

Hemodynamic force does not impact the total number of vSMCs available

Since there could still be undetectable differences in vSMC differentiation, this could affect the total amount of vSMCs available to cover vessels, even if the vSMC proliferation rates are the same. For example, if one tissue starts off with 8 vSMCs, and another with 10 vSMCs, if all parent and daughter cells divide three times, the first tissue will have ~ 512 vSMCs, and the second would have 1000 vSMCs—nearly double the amount. Thus, I wanted to determine if reduced-flow embryos and yolk sacs have a lower total amount of vSMCs than in normal-flow yolk sacs. Using microscopy, it is impossible to visually quantify the total number of vSMCs because of the overlap around proximal arteries and veins. Thus, to measure if there was a total change of vSMC affected by low hemodynamic force, flow cytometry with the Sma antibody was used (Fig. 1).

Measurements were taken by counting the total number of vSMCs (Sma+ cells) divided by the total number of embryo or yolk sac cells that flow through the cytometer. This allows for accurate comparisons between tissues that may not be the exact same size.

Normal-flow and reduced-flow tissue from whole embryos were compared and no significant difference in the amount of vSMCs was observed (Fig, 6). Similarly, no significant difference in the total amount of vSMCs was found when comparing yolk sac tissue (Fig. 6). In summary, hemodynamic force does not impact the total number of vSMCs available for vessel coverage. I reasoned, therefore, that a factor other than hemodynamic force explain why reduced-flow vessels fail to acquire a vSMC layer.

Hemodynamic force affects the recruitment of vSMCs from capillary region to proximal vessels

Based on my observations that hemodynamic force did not impact the total number of vSMCs available, I speculated that hemodynamic force did not affect the ability for vSMCs to differentiate from the mesoderm, or to exhibited altered proliferation. Instead, vSMCs failed to be recruited from the surrounding capillary region towards the proximal arteries and veins (Fig. 2). To assess if recruitment is impaired by reduced-flow, *Myl7;CD1-Tg(sma-mCherry)* with *Sma-myr::mCherry* transgenic mouse yolk sac were used to assess an area analysis of the space occupied by vSMC in the capillary regions. The premise behind this analysis is that in normal-flow yolks sacs, vSMCs differentiate and proliferate normally in the capillary regions, and they migrate towards the larger, high-flow proximal vessels. In reduced-flow, on the other hand, I speculate that the cells do not migrate to the proximal vessels (because they have low-

flow). As a result, I anticipate visualizing more vSMCs in the capillary regions of reduced-flow yolk sacs.

Capillary regions of normal-flow yolk sacs showed that there were vSMCs present (Fig. 7A-D). However, in the capillary regions of reduced-flow yolk sacs, there was an increase in the amount of vSMCs present (Fig. 7E-H). After binarization and area analysis, there was a significant increase in the amount of area occupied by vSMCs in low hemodynamic force capillary regions relative to the normal flow capillary regions (Fig. 7I). Thus, this suggests that hemodynamic force promotes the recruitment of vSMCs to vessels of high-flow.

DISCUSSION

Adult vessels that are located closer to the heart (proximally) have a thicker tunica media layer relative to vessels closer to the extremities (distally) (Isayama et al., 2013). Vessels closer to the heart are subjective to much stronger hemodynamic forces and must have a thicker vascular smooth muscle layer to counteract those forces. Data produced by this study supports that differences in tunica media thickness are established during embryonic development, and that hemodynamic force is the key regulator for vSMC coverage. Results demonstrate that the cellular mechanism of hemodynamic force-induced vascular maturation involves the recruitment of vSMCs from the capillary regions towards the proximal arteries and veins, and this does not occur by a localized vSMC proliferation/differentiation mechanism.

In normal-flow mouse embryos, our results revealed noticeable differences in vSMC coverage in different vessel subtypes, with highest coverage in proximal arteries, followed by a progressively reduced coverage in proximal veins and capillaries. This reduction is likely due to the differences during development in the amount of hemodynamic force that the developing vessels are exposed to. For example, proximal arteries in the mouse yolk sac are subjected to the strongest forces, as blood leaving the embryo enters into the yolk sac (McGrath et al., 2003); (Udan et al., 2013). Upon the distribution of the blood into numerous capillaries, hemodynamic force diminishes. As blood collects in the proximal vein is carried blood away from the yolk sac back to the embryonic heart, the hemodynamic force increases but will not the level found in proximal arteries. These differences in force correlate well with differences in vSMC

coverage, implicating that extent of hemodynamic force determines the amount of vSMC coverage. Indeed, hemodynamic force is required for proper maturation, as our data in reduced-flow embryos reveals diminished or an absent vSMC coverage, even around proximal arteries.

Given the correlation of the amount of force and the extent of vSMC coverage, I propose a model where hemodynamic force acts like an analog signal, rather than a digital signal. Thus, force induces a gradient of recruitment signaling of vSMCs, as oppose to an on-and-off signaling mechanism. The wide variety in thickness of tunica media lends support to this model. There is no set amount of thickness for a given vessel and there is a variation throughout an organism (Dinardo et al., 2014).

A recently published study reached a similar conclusion, and proposed that hemodynamic force regulated mural cell coverage in blood vessels (Chen et al., 2017). Using zebrafish embryos, the Santoro lab proposed a mechanism where blood vessel endothelial cells possess non-motile cilia that deflect upon exposure to hemodynamic force. This, in turn upregulates *Notch* and *Foxc1b* expression to encourage mural cell recruitment. Based on evidence that our lab and others have collected, it appears as if there is partial conservation of this pathway in the mouse. What is not conserved is the role of non-motile cilia. These cilia are not detected in mouse yolk sac vessels (personal communication with Mary Dickinson, Baylor College of Medicine). What does appear to be conserved is the Notch pathway, which I have observed is downregulated in reduced-flow mouse embryos (data not shown). However, more studies need to be done to validate the role of Notch in vSMC recruitment, and to determine the role of the *FoxC1* gene in vascular maturation of the mouse. Though the Santoro lab has provided insight

into the molecular mechanisms of vSMC coverage, the investigators did not assess whether increased coverage occurs via vSMC recruitment or localized vSMC proliferation/differentiation.

The mechanism of how high-flow, proximal vessels signal the recruitment of vSMCs remains unknown. One possible mechanism is that high-flow vessels recruit vSMCs via chemotaxis towards a paracrine factor. For example, vessels that are exposed to high hemodynamic force could induce Notch activation. This, in turn, could upregulate expression of a paracrine factor, and vSMCs will migrate in the direction towards the highest concentration of the paracrine factor. In another possible mechanism, maturation occurs via a juxtacrine pathway. Perhaps, vSMCs randomly migrate throughout the yolk sac, but they only adhere to vessels that express adhesion factors, like cadherins or gap junction molecules. In this scenario, vSMCs only adhere to high-flow vessels which express a high amount of adhesion molecules.

To determine which mechanism occurs, live imaging and cell tracking studies will be performed. However, it is challenging to visualize vSMC recruitment over time in mice. vSMCs differentiate at around E9.5, and the culturing mouse embryos beyond this point is challenging. Thus, in future studies, confocal imaging will be performed using E9.5 embryos that will be cultured only for several hours (instead of overnight). Though several problems need to be overcome (setting up the confocal for live embryo culture, determining whether excitation light will allow for visualization but will not photodamage the embryo, and ensuring that the culturing time is sufficient to visualize migration), the ultimate goal will be to visualize if vSMCs stream towards proximal

vessels, or if they undergo random migration, but stick to the proximal vessel when nearby.

Though the studies of this thesis represent basic science, my findings could have significant applicability for human health and medicine. By ultimately discovering the mechanism for vSMC recruitment, this information could be used to control vSMC recruitment in adult vessels that are depleted of the tunica media (perhaps caused by a congenital defect, injury, or environmental factors). For example, aneurysms are regions of a blood vessel that have a weak vessel wall, partly caused by the degradation of the tunica media that are prone to ballooning and potentially hemorrhaging. Currently, stents are used to repair cardiovascular aneurysms, however, many patients experience repeated aneurysm events, leading to a reduced lifespan (Lederle et al., 2012). Since stents can be used to deliver localized treatment by seeding with a drug (Giap, 2002), stents could be seeded with discovered factors to encourage vSMCs to be recruited to the thin vessel walls. It is possible that adult vSMCs will respond in a way similar to the embryonic vSMCs response, because they are capable of reverting to an embryonic-like vSMC (a process called phenotypic modulation) where they are capable of partial dedifferentiation, proliferation, migration, and redifferentiation (Rensen et al., 2007). In summary, results from my basic science research could point in the direction of possible clinical advances.

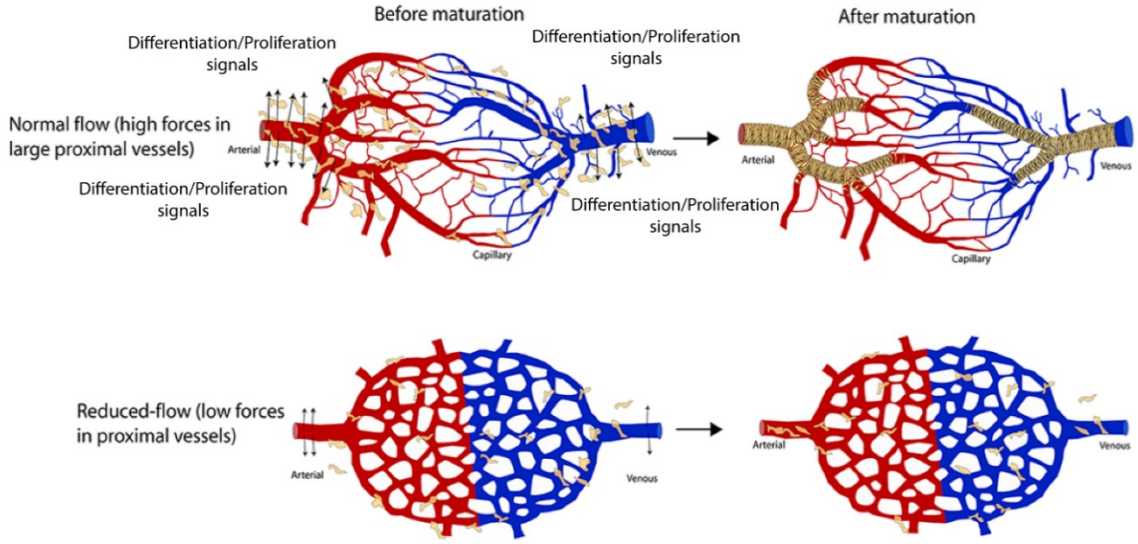

Figure 1. Hypothesis 1: Hemodynamic force promotes the localized proliferation and/or differentiation of vSMCs. In normal-flow yolk sacs, areas of high hemodynamic force, including the proximal arteries and veins, secrete differentiation and/or proliferation signals to promote the localized differentiation and/or proliferation of vSMCs; whereas, the distal capillaries with low hemodynamic force would have fewer vSMCs. In this model, vSMCs are limited in the ability to migrate around the yolk sac, so they wrap around the nearest vessels, resulting in a higher amount in proximal vessels. If hemodynamic force is reduced throughout the entire yolk sac, the expected phenotype would be a reduction in vSMCs in proximal vessels, as well as a reduction in the distal capillaries. Figure modified from Udan et al., 2013a.

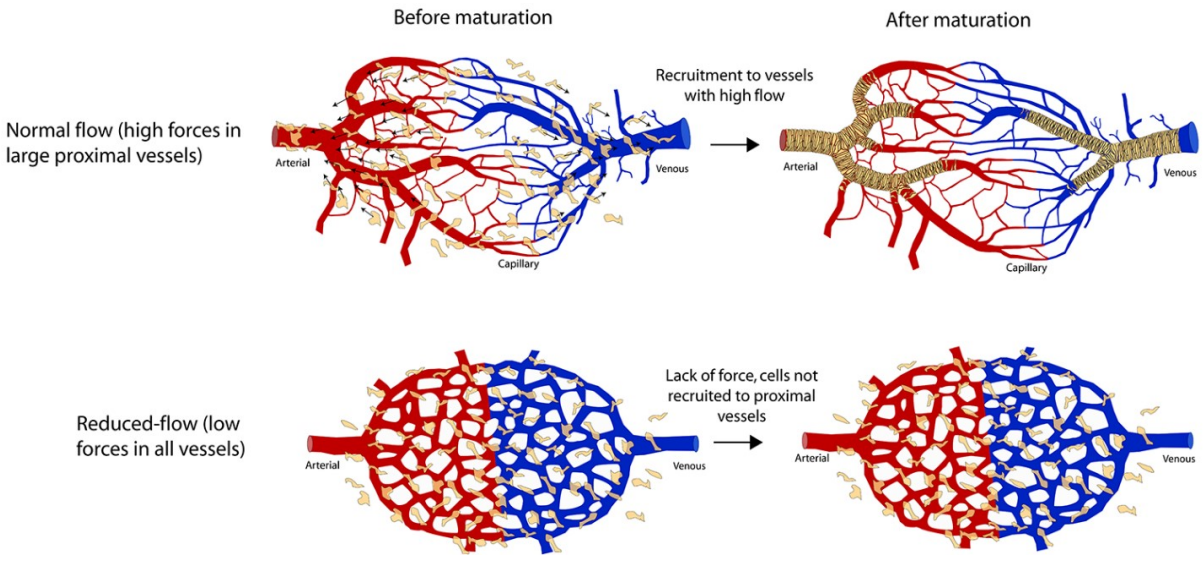

Figure 2. Hypothesis 2: Hemodynamic force promotes the recruitment of vSMCs. In normal-flow yolk sacs, vSMCs are capable of differentiating evenly throughout the entire yolk sac. However, proximal vessels with higher hemodynamic force promote the recruitment of vSMCs from distal capillaries with lower hemodynamic force. If hemodynamic force is reduced throughout the entire yolk sac, there will be an absence of recruitment signals, but there will be no change in the overall amount of vSMCs available. Thus, the expected phenotype would be the appearance of a greater amount of unbound vSMCs (vSMCs that fail to recruit and surround vessels) in distal capillary regions. Figure modified from Udan et al., 2013a.

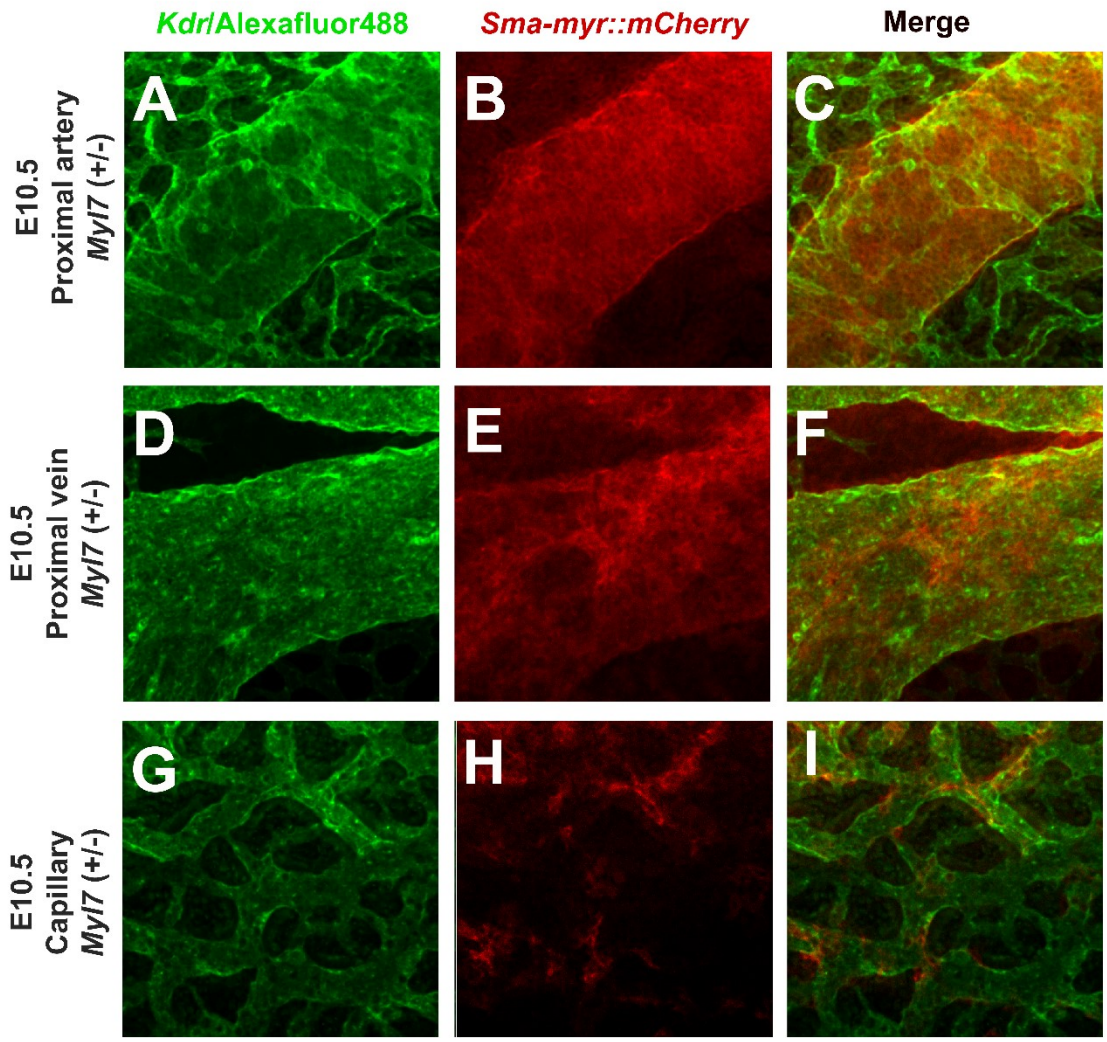

Figure 3. Proximal arteries exhibit greater vSMC coverage than proximal veins and distal capillaries. Whole mount embryonic mouse yolk sacs were labeled with endothelial cell (Kdr/Flk1:Alexa Fluor488) and vSMC cell (Sma-myr::mCherry) markers to display the proximal artery, proximal vein, and distal capillaries in a normal-flow yolk sac. The artery shows complete vSMC coverage around the vessel, which is comprised on endothelial cells (A-C). In comparison, the vein shows vSMC coverage around the vessel, however, vSMC coverage is sparse when compared to the artery (D-F). The capillary region of the yolk sac (G-I) shows the most significant reduced coverage, as only individual vSMCs are found around the endothelium.

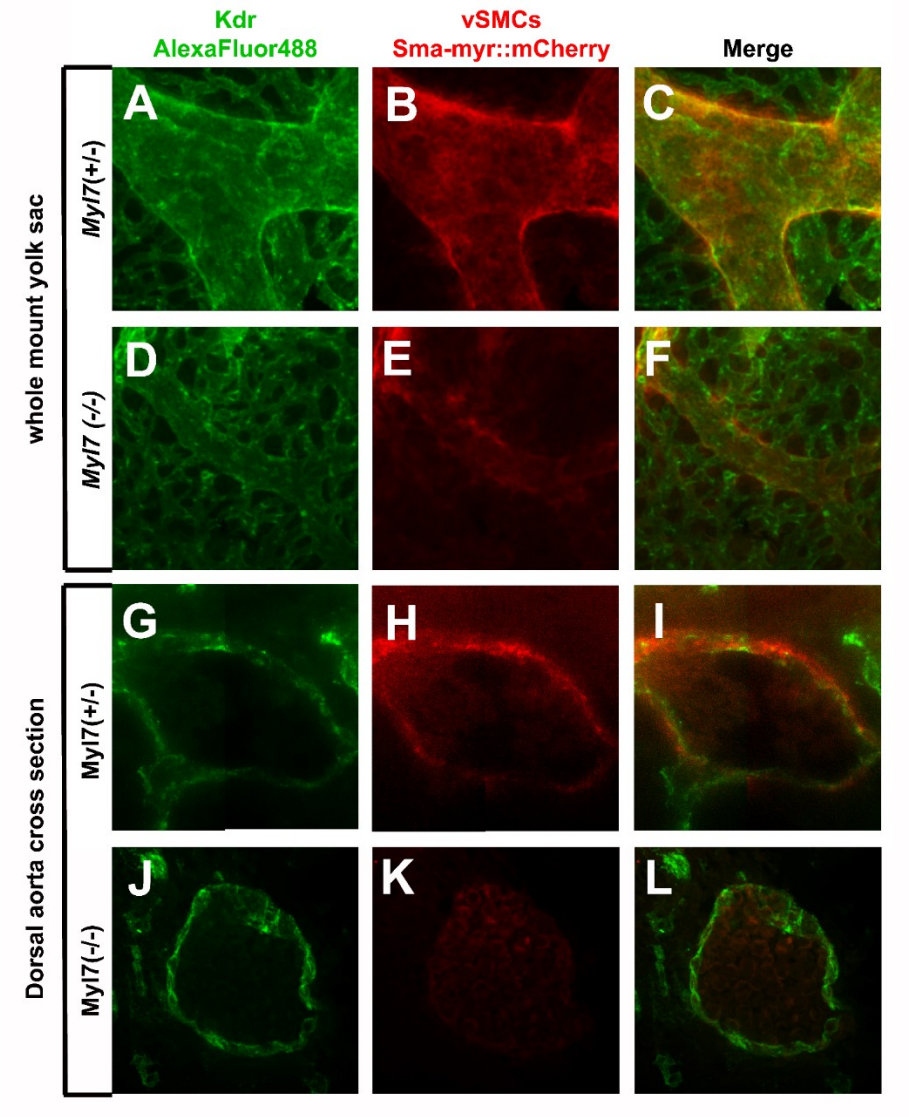

Figure 4. Vascular smooth muscle layer is reduced in low hemodynamic force. Embryonic whole mount yolk sac and dorsal aorta cross section tissue were labeled with endothelial cell (Kdr/Flk1:Alexa Fluor488) and vSMC cell (Sma-myr::mCherry) markers. vSMC coverage is reduced in *Myl7* (-/-) reduced-flow proximal arteries (D-F) when compared to *Myl7* (+/-) normal-flow proximal arteries (A-C). This was also observed in intraembryonic tissues, as the cross sections of the dorsal aorta of normal-flow embryos displayed high vSMC coverage (G-I); whereas, the dorsal aorta of reduced-flow embryos exhibited diminished/absent vSMC coverage (J-L).

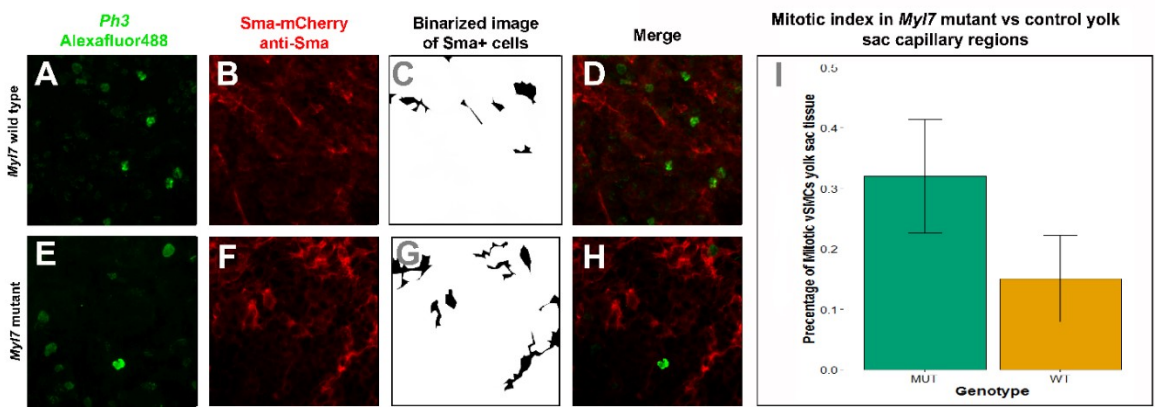

Figure 5. Low hemodynamic force does not impact the proliferation and differentiation of vSMCs. Representative images of E10.5 *Myl7* wild-type (normal-flow) yolk sacs (A-D) and *Myl7* mutant (reduced-flow) yolk sacs (E-H). Yolk sacs were labeled with phosho-histone H3 (PH3) and Alexa Fluor488 antibodies (mitotic marker) and *Sma-myr::mCherry* (Sma) smooth muscle marker. The total number of PH3, Sma double positive cells were divided by the total surface area occupied by Sma-labeled cells to develop the mitotic index. Comparison of the mitotic index between the normal-flow and reduced-flow yolk sacs reveal no significant difference (I). Statistical significance was calculated using standard error, $p < 0.05$.

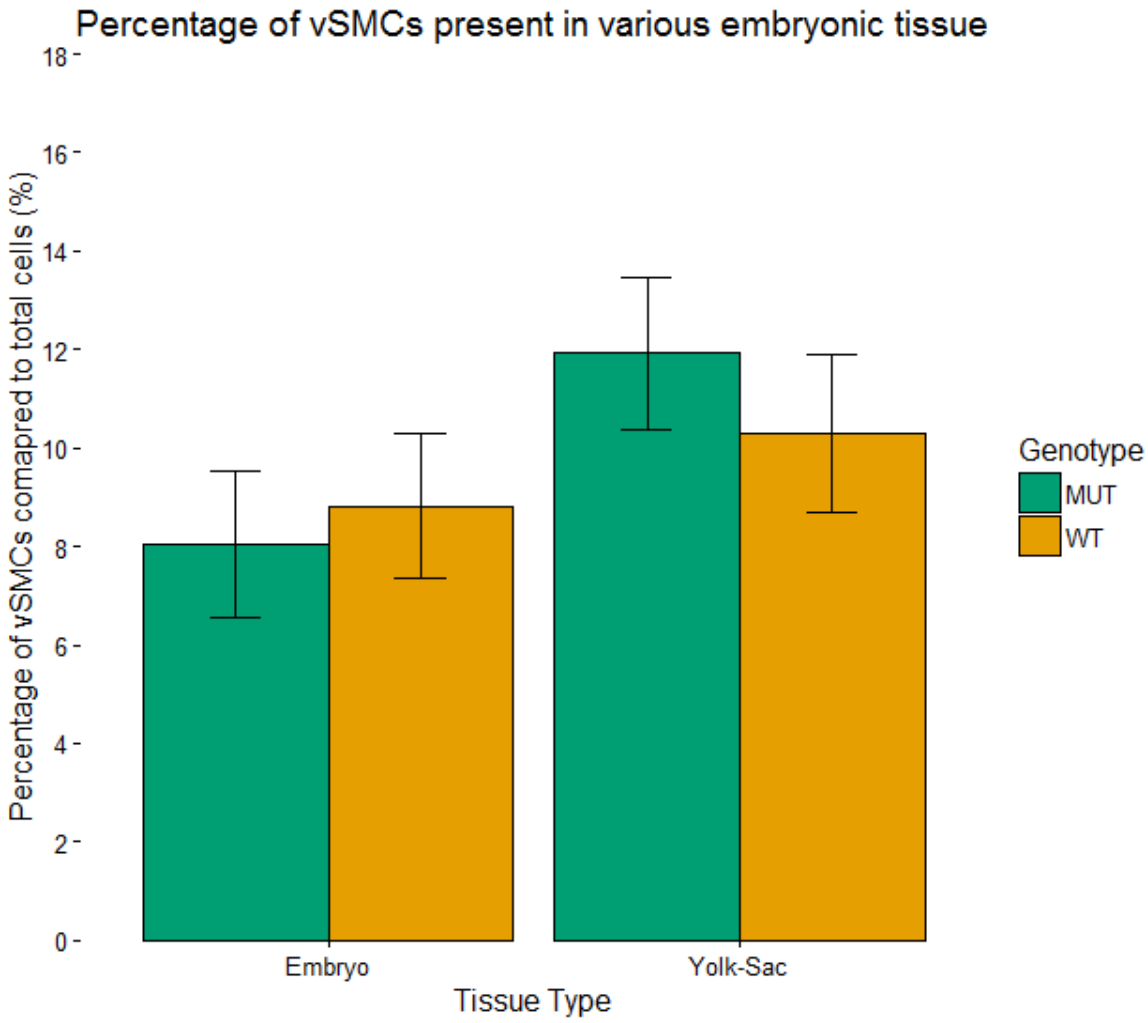

Figure 6. Total number of vSMCs is not impacted by low hemodynamic force. Flow cytometry analysis, using the *Sma-myr::mCherry* smooth muscle marker to label vSMCs, revealed that the total number of vSMCs is not significantly different between normal-flow or reduced-flow embryonic or yolk sac tissue. Statistical significance was calculated using standard error, $p < 0.05$.

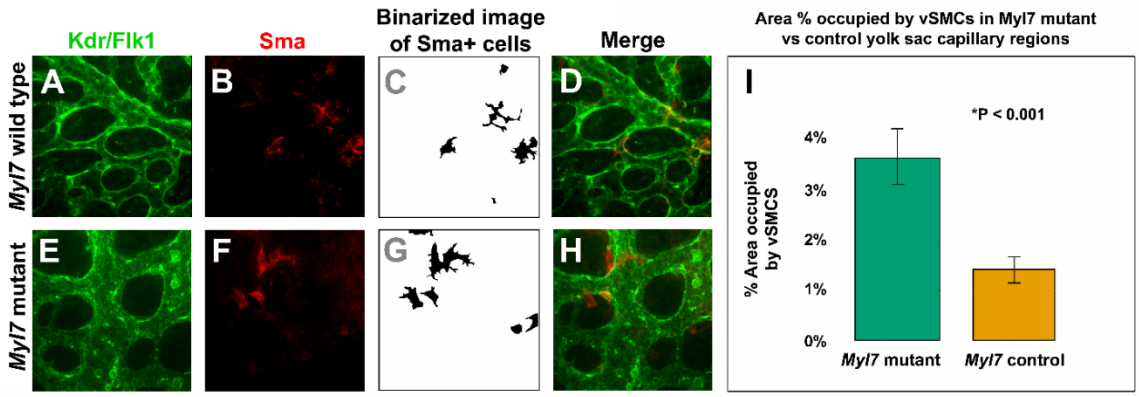

Figure 7. Recruitment of vSMCs from capillary region is impaired in low hemodynamic force yolk sacs. Representative images of distal capillary regions of *Myl7* wild-type (normal-flow) yolk sacs (A-D) and *Myl7* mutant (reduced-flow) yolk sacs (E-H). Yolk sacs were labeled with Kdr/Flk1:Alexa Fluor488 endothelial marker and *Sma-myr::mCherry* smooth muscle marker. *Myl7* mutant yolk sacs displayed significantly ($P<0.001$) increased vSMC area coverage when compared to *Myl7* wild-type capillary regions (I).

REFERENCES

Armstrong, J.J., Larina, I.V., Dickinson, M.E., Zimmer, W.E., Hirschi, K.K. (2010). Characterization of Bacterial Artificial Chromosome Transgenic Mice Expressing mCherry Fluorescent Protein Substituted for The Murine Smooth Muscle Alpha-Actin Gene. Genesis (New York, N.Y. : 2000) 48, 457-463.

Armulik, A., Genove, G., Betsholtz, C. (2011). Pericytes: developmental, physiological, and pathological perspectives, problems, and promises. Dev Cell 21, 193-215.

Barron, M.R., Belaguli, N.S., Zhang, S.X., Trinh, M., Iyer, D., Merlo, X., Lough, J.W., Parmacek, M.S., Bruneau, B.G., Schwartz, R.J. (2005). Serum Response Factor, an Enriched Cardiac Mesoderm Obligatory Factor, Is a Downstream Gene Target for Tbx Genes. Journal of Biological Chemistry 280, 11816-11828.

Chen, X., Gays, D., Milia, C., Santoro, M. (2017). Cilia Control Vascular Mural Cell Recruitment in Vertebrates. Cell Reports 18, 1033-1047.

Corada, M., Morini, M.F., Dejana, E. (2014). Signaling pathways in the specification of arteries and veins. Arterioscler Thromb Vasc Biol 34, 2372-2377.

D'Alessio, A., Moccia, F., Li, J.H., Micera, A., Kyriakides, T.R. (2015). Angiogenesis and Vasculogenesis in Health and Disease. Biomed Res Int 2015, 126582.

Dinardo, C.L., Venturini, G., Zhou, E.H., Watanabe, I.S., Campos, L.C.G., Dariolli, R., da Motta-Leal-Filho, J.M., Carvalho, V.M., Cardozo, K.H.M., Krieger, J.E., Alencar, A.M., Pereira, A.C. (2014). Variation of mechanical properties and quantitative proteomics of VSMC along the arterial tree. American Journal of Physiology - Heart and Circulatory Physiology 306, H505-H516.

Drake, C.J., Fleming, P.A. (2000). Vasculogenesis in the day 6.5 to 9.5 mouse embryo. Blood 95, 1671-1679.

Eerola, I., Boon, L.M., Mulliken, J.B., Burrows, P.E., Dompmartin, A., Watanabe, S., Vanwijck, R., Vikkula, M. (2003). Capillary Malformation–Arteriovenous Malformation, a New Clinical and Genetic Disorder Caused by RASA1 Mutations. The American Journal of Human Genetics 73, 1240-1249.

Ferguson, J.E., 3rd, Kelley, R.W., Patterson, C. (2005). Mechanisms of endothelial differentiation in embryonic vasculogenesis. Arterioscler Thromb Vasc Biol 25, 2246-2254.

Ferrer-Vaquer, A., Viotti, M., Hadjantonakis, A.-K. (2014). Transitions between epithelial and mesenchymal states and the morphogenesis of the early mouse embryo. Cell Adhesion & Migration 4, 447-457.

Gaengel, K., Genove, G., Armulik, A., Betsholtz, C. (2009). Endothelial-mural cell signaling in vascular development and angiogenesis. Arterioscler Thromb Vasc Biol 29, 630-638.

Giap, H., 2002. Required treatment margin for coronary endovascular brachytherapy with iridium-192 seed ribbon. Cardiovascular Radiation Medicine 3, 49-55.

Herbert, S.P., Stainier, D.Y.R. (2011). Molecular control of endothelial cell behaviour during blood vessel morphogenesis. Nat Rev Mol Cell Biol 12, 551-564.

Huang, C., Sheikh, F., Hollander, M., Cai, C., Becker, D., Chu, P.H., Evans, S., Chen, J. (2003). Embryonic atrial function is essential for mouse embryogenesis, cardiac morphogenesis and angiogenesis. Development 130, 6111-6119.

Ichikawa, T., Nakazato, K., Keller, P.J., Kajiura-Kobayashi, H., Stelzer, E.H., Mochizuki, A., Nonaka, S. (2013). Live imaging of whole mouse embryos during gastrulation: migration analyses of epiblast and mesodermal cells. PLoS One 8, e64506.

Isayama, N., Matsumura, G., Yamazaki, K. (2013). Comparison of vascular smooth muscle cells in canine great vessels. BMC Veterinary Research 9, 54.

Jabari, S., Hartmann, A., Cesnjevar, R. (2016). A rare case of congenital thoracic arteriovenous fistula between the brachiocephalic truncus and the superior vena cava resulting in heart failure. Journal of Pediatric Surgery Case Reports 15, 50-52.

Jacot, J.G., Wong, J.Y. (2008). Endothelial injury induces vascular smooth muscle cell proliferation in highly localized regions of a direct contact co-culture system. Cell Biochem Biophys 52, 37-46.

Jones, E.A.V., Yuan, L., Breant, C., Watts, R.J., Eichmann, A. (2008). Separating genetic and hemodynamic defects in neuropilin 1 knockout embryos. Development 135, 2479-2488.

Kakarla, U.K., Beres, E.J., Ponce, F.A., Chang, S.W., Deshmukh, V.R., Bambakidis, N.C., Zabramski, J.M., Spetzler, R.F. (2010). Microsurgical Treatment of Pediatric Intracranial Aneurysms: Long-term Angiographic and Clinical Outcomes. Neurosurgery 67, 237-250.

Korn, C., Augustin, H.G. (2015). Mechanisms of Vessel Pruning and Regression. Dev Cell 34, 5-17.

Kovacic, J.C., Mercader, N., Torres, M., Boehm, M., Fuster, V. (2012). Epithelial-to-mesenchymal and endothelial-to-mesenchymal transition: from cardiovascular development to disease. Circulation 125, 1795-1808.

Kurz, H., Burri, P.H., Djonov, V.G. (2003). Angiogenesis and Vascular Remodeling by

Intussusception: From Form to Function. Physiology 18, 65-70.

le Noble, F., Moyon, D., Pardanaud, L., Yuan, L., Djonov, V., Matthijsen, R., Bréant, C., Fleury, V., Eichmann, A. (2004). Flow regulates arterial-venous differentiation in the chick embryo yolk sac. Development 131, 361-375.

Lederle, F.A., Freischlag, J.A., Kyriakides, T.C., Matsumura, J.S., Padberg, F.T.J., Kohler, T.R., Kougias, P., Jean-Claude, J.M., Cikrit, D.F., Swanson, K.M. (2012). Long-Term Comparison of Endovascular and Open Repair of Abdominal Aortic Aneurysm. New England Journal of Medicine 367, 1988-1997.

Liberthson, R.R., Sagar, K., Berkoben, J.P., Weintraub, R.M., Levine, F.H. (1979). Congenital coronary arteriovenous fistula. Report of 13 patients, review of the literature and delineation of management. Circulation 59, 849-854.

Lucitti, J.L., Jones, E.A., Huang, C., Chen, J., Fraser, S.E., Dickinson, M.E. (2007). Vascular remodeling of the mouse yolk sac requires hemodynamic force. Development 134, 3317-3326.

Mack, C.P. (2011). Signaling Mechanims That Regulate Smooth Muscle Cell Differentiation. Arteriosclerosis, Thrombosis, and Vascular Biology 31, 1495-1505.

McGrath, K.E., Koniski, A.D., Malik, J., Palis, J. (2003). Circulation is established in a stepwise pattern in the mammalian embryo. Blood 101, 1669-1675.

Mokalled, M.H., Carroll, K.J., Cenik, B.K., Chen, B., Liu, N., Olson, E.N., Bassel-Duby, R. (2015). Myocardin-related transcription factors are required for cardiac development and function. Developmental Biology 406, 109-116.

Moore, M.A.S., Metcalf, D. (1970). Ontogeny of the Haemopoietic System: Yolk Sac Origin of In Vivo and In Vitro Colony Forming Cells in the Developing Mouse Embryo*. British Journal of Haematology 18, 279-296.

Rensen, S.S.M., Doevendans, P., van Eys, G. (2007). Regulation and characteristics of vascular smooth muscle cell phenotypic diversity. Netherlands Heart Journal 15, 100-108.

Schmidt, A., Brixius, K., Bloch, W. (2007). Endothelial precursor cell migration during vasculogenesis. Circ Res 101, 125-136.

Shin, D., Garcia-Cardena, G., Hayashi, S., Gerety, S., Asahara, T., Stavrakis, G., Isner, J., Folkman, J., Gimbrone, M.A., Jr., Anderson, D.J. (2001). Expression of ephrinB2 identifies a stable genetic difference between arterial and venous vascular smooth muscle as well as endothelial cells, and marks subsets of microvessels at sites of adult neovascularization. Dev Biol 230, 139-150.

Sorteberg, A., Dahlberg, D. (2013). Intracranial Non-traumatic Aneurysms in Children

and Adolescents. Current Pediatric Reviews 9, 343-352.

Tammela, T., Zarkada, G., Nurmi, H., Jakobsson, L., Heinolainen, K., Tvorogov, D., Zheng, W., Franco, C.A., Murtomaki, A., Aranda, E., Miura, N., Yla-Herttuala, S., Fruttiger, M., Makinen, T., Eichmann, A., Pollard, J.W., Gerhardt, H., Alitalo, K. (2011). VEGFR-3 controls tip to stalk conversion at vessel fusion sites by reinforcing Notch signalling. Nat Cell Biol 13, 1202-1213.

Udan, R.S., Culver, J.C., Dickinson, M.E. (2013a). Understanding vascular development. Wiley Interdiscip Rev Dev Biol 2, 327-346.

Udan, R.S., Vadakkan, T.J., Dickinson, M.E. (2013b). Dynamic responses of endothelial cells to changes in blood flow during vascular remodeling of the mouse yolk sac. Development 140, 4041-4050.

van Rooij, W.J., Sluzewski, M. (2009). Endovascular treatment of large and giant aneurysms. AJNR Am J Neuroradiol 30, 12-18.

You, L.R., Takamoto, N., Yu, C.T., Tanaka, T., Kodama, T., Demayo, F.J., Tsai, S.Y., Tsai, M.J., 2005. Mouse lacking COUP-TFII as an animal model of Bochdalek-type congenital diaphragmatic hernia. Proc Natl Acad Sci U S A 102, 16351-16356.